Modelling Lifted Methane Jet Fires Using the Boundary Layer Equations

By P.S. Cumber[1*] and M. Spearpoint[**]

Heriot-Watt University[*]
School of Engineering and Physical sciences
Riccarton Campus
Edinburgh
United Kingdom

Dept of Civil Engineering[**]
University of Canterbury
Private Bag 4800
Christchurch 8020
New Zealand

Abstract

The focus of this paper is turbulent lifted jet fires. The main objective is to present a lifted jet fire methodology using the boundary layer equations as a basis. The advantages of this are finite volume mesh independent predictions of the mean flow fields can be calculated on readily available computer resources which leads to rigorous model calibration. A number of lift-off models are evaluated. The model of choice is one based on the laminar flamelet quenching concept combined with a model for the large-scale strain rate.

KEYWORDS: lifted jet fires, parabolic flow model, flamelet quenching, strain rate modelling, combustion

---
[1] Corresponding author: E-Mail Address p.s.cumber@hw.ac.uk

Nomenclature

C_1, C_2, C_μ	Parameters in the k-ε turbulence model
$C_{p,i}$	Specific heat of species i
$C_{s,1}$, $C_{s,2}$	Calibration constants in strain rate models
d	Nozzle diameter
f	Mixture fraction
$f^{"2}$	Variance of mixture fraction
k	Turbulence kinetic energy
K_a	Absorption coefficient
l_t	Turbulence length scale
P	Turbulence production source term, Probability density function
P_b	Probability of burning
P_{burn}	Composite probability of burning
P_c	Percolation threshold
P_d	Probability of burning relating to the location of the fluctuating flame base
q_{Rad}	Radiation heat flux
r	Radial co-ordinate
r_{st}	Radial location of the stoichiometric concentration
s	Strain rate
T	Temperature
U	Stream-wise velocity
U_0	Source velocity
V	Radial velocity
Y_i	Mass fraction of species i
z	Axial co-ordinate
z_L	Lift-off height

Greek Symbols:

Δh	Enthalpy perturbation
ε	Dissipation rate of turbulence kinetic energy

φ	Generic flow variable
φ_b	Burning flamelet
φ_m	Isothermal mixing flamelet
κ	Von Karman Constant
μ_{eff}	Effective viscosity
μ_l	Laminar viscosity
μ_t	Turbulent viscosity
ν_l	Kinematic viscosity
ρ	Density
σ	Stefan Boltzmann constant
$\sigma_{\Delta h}$	Turbulent Prandtl number for specific enthalpy perturbation
σ_ε	Turbulent Prandtl number for the dissipation rate of turbulence kinetic energy
σ_k	Turbulent Prandtl number for the turbulence kinetic energy

Subscripts:

adia	Adiabatic property
amb	Ambient value
q	Quench value
st	Property at stoichiometric conditions
0	Initial condition or source condition

Over bars

-	Reynolds averaged quantity
~	Favre averaged quantity

Introduction

Turbulent jet flames occur in many areas of industry either by accident such as following the ignition of a leak from a high pressure plant processing hydrocarbons or in a controlled environment such as a furnace or industrial burner. In a turbulent jet the flow is characterised by the diameter of the nozzle or pipe, the fuel composition and the speed of the fuel at the nozzle exit. For a given fuel and nozzle diameter, if the jet speed is sufficiently low the flame is attached or rim-stabilised. If the jet speed is gradually increased then at some critical velocity the jet lifts off and the flame structure fundamentally changes. Immediately downstream of the nozzle the flow is non-reacting, further downstream combustion is initiated at a fluctuating flame base followed by the main body of the jet flame. For most fuels and nozzle diameters the critical velocity is relatively low, for example, [1] give a critical velocity of 15.4 m/s for a propane jet fire with a nozzle diameter of 8.74 mm. Therefore the understanding of lifted jet fires is of interest to industrial combustion engineers. A wide range of small-scale [2-5] and large-scale experimental and theoretical studies of lifted fires [6-8] exist in the open literature. In some situations lifted flames are encouraged as it has been shown that lifted flames can reduce NO_x levels in furnaces, [9].

The computational modelling of rim-stabilised fires is mature with good agreement between the predicted and measured mean temperature and major chemical species established, [10-12]. This is not the case for lifted jets where computational studies have focussed on understanding the mechanism for the location of the combusting flame base and good agreement between predicted and measured flow properties is not universal. The possible mechanisms for the location of the lift-off height will be considered further below. Where turbulence-radiation effects are small, which has been shown to be the case for laboratory scale methane jets [11], predicted received radiation heat fluxes surrounding a rim-stabilised fire are in reasonable agreement with measured fluxes [11,13,14], whereas for lifted fires this as yet has not been considered seriously.

The mechanism for flame lift-off is a competition between chemical and mixing processes characterised by a chemical reaction time and a flow residence time. The

ratio of these time-scales is defined as the Damköhler number. As the jet velocity increases the flow residence time decreases. At the critical velocity or Damköhler number there is insufficient time for the chemical reaction to take place and lift-off occurs, [4]. This is the accepted physical explanation for flame lift-off but the mechanism involved in flame stabilisation at the lift-off height after over three decades of research is still debated vigorously. The early accepted theory was the lift-off height was determined by the downstream location on the stoichiometric contour where the mean jet velocity equals the turbulent burning velocity. The location of the flame base is governed by the premixed nature of the fuel air mixture. Computational models using this criterion were able to predict lift-off heights for the jet fires considered [15]. Experimentalists were also able to correlate measured lift-off heights for a range of fuels using the premixed assumption and the turbulent burning velocity, [2].

Peters and Williams [16] were the first to question this theory suggesting that insufficient premixing could occur for the premixed theory to be valid in the lifted jet fires they considered. Peters and Williams based their analysis on Pitts [17] experiments, proposing another mechanism, based on laminar flamelet quenching that relies on an analysis of laminar flamelets distorted by the turbulence field. At the fluctuating flame base the lifted flame can be considered as an ensemble of laminar flamelets in the instantaneous field; the laminar flamelets varying from air-fuel mixtures at or near stoichiometric conditions to fully entrained air. Each of the flamelets can be considered to be burning or non-reacting depending on the local instantaneous composition and level of turbulent distortion or stretch the flamelet is subjected to. The location of the flame base is determined by the proportion of burning to non-reacting flamelets. A candidate property for characterising the degree of stretch of the flamelets is the scalar dissipation rate, [18], although Sanders and Lamers [4] present a convincing argument against the scalar dissipation rate and suggest the strain rate as the appropriate parameter. Muller et al. [5] use a model for the strain rate of the largest eddies to predict the lift-off height, whereas Sanders and Lamers favour the small-scale strain rate. Sanders and Lamers base their conclusions on a calibration of lift-off height using isothermal simulations, the argument being the lift-off height is primarily determined by the flow upstream of the flame base. As well as the two theories discussed above Pitts [3] analysed a number of lifted jet fires and

suggests that the location of the lift-off height is determined by large-scale rather than small-scale structures in the jet, and isothermal mixing upstream of the lift-off region is important in determining the location of the flame base. Even though Pitts presents a compelling case for his favoured mechanism he still states that models based on a premixed theory or small-scale turbulent structures can not be discounted. More recently Upatnicks et al. [19] using a high speed photography technique, Cinema PIV identified another mechanism for the location of the lift-off height based on an analysis of the edge of the flame. One reason for the lack of clarity as to the correct mechanism is all theories show some degree of agreement with observation, and in many experiments there is considerable overlap in prerequisite conditions for each theory to apply.

In this paper a model originally proposed by Sanders and Lamers [4] based on the laminar flamelet quenching concept is implemented although the conclusion as to the appropriate scale of the strain rate model differs from Sanders and Lamers. The main objective of this paper is to present a lifted jet fire methodology based on a parabolic flow model and as such the use of laminar flamelet quenching is a convenient lift-off model. The methodology presented with minor modification could be implemented with other lift-off models. The overall computational framework is a parabolic flow solver, utilising the boundary layer equations, similar to GENMIX, [20], extended to include elliptic features found in lifted fires. In lifted jet fires the important elliptic features are the feedback mechanisms downstream of the lift-off region that determines the lift-off height and local flame structure. In the context of the lift-off model implemented here, Sanders and Lamer's model, [4], the elliptic feedback mechanism is introduced through the probability of burning field. The details of implementation are considered further below. As jet fires have a dominant flow direction it is common for the flame structure of a rim-stabilised jet fire to be calculated in this way, [10-12]. This is the first time lifted flame predictions based on a parabolic flow model have been reported. The computational advantages of a parabolic flow model over a fully elliptic solver are clear, as no iteration cycle of a pressure correction algorithm is required in its solution as the dominant flow direction has a time like quality allowing a marching procedure in the dominant flow direction. This makes it possible to calculate complex flame structures using readily available computational resources. For example Wang and Chen, [21] have recently reported

the computation of a laboratory scale rim-stabilised flame, Flame D in ref. [22]; the simulation is calculated using a PDF transport model with detailed chemistry, including 53 species and 32 elemental reactions and a multi-time-scale k-ε turbulence model. Either of these modelling approaches in isolation would make the jet fire calculation prohibitively computationally intensive when combined with an elliptic solver on a standard PC. Using a flow solver based on the boundary layer equations Wang and Chen report a run-time of the order of 1 week on a relatively high specification PC. The use of a parabolic solver is not only an issue of convenience as it makes it relatively simple to demonstrate mesh independence in any predicted flow fields presented. In addition any model calibration is purely dependent on the quality of the experimental data used in the calibration. The issue of robust calibration is a particularly important one as without it, model development looses rigour. In this paper the final issue addressed is the received radiation heat flux distributions sensitivity to the representation of the lift-off region.

In the next section the mathematical model is presented. The details for the most part follow Sanders and Lamers [4] formulation but differs in a number of key areas. The model basis as described by Sanders and Lamers is repeated here for completeness and convenience.

Mathematical Model

The basis of the flow equations is the parabolized Favre averaged Navier Stokes equations in an axisymmetric coordinate system. The system is closed using a variant of the k-ε turbulence model.

$$\frac{\partial \overline{\rho} \widetilde{U} k}{\partial z} + \frac{1}{r}\frac{\partial r\overline{\rho}\widetilde{V} k}{\partial r} = \frac{1}{r}\frac{\partial}{\partial r}\left(r\frac{\mu_{eff}}{\sigma_k}\frac{\partial k}{\partial r}\right) + \overline{\rho}\left(P - \varepsilon\right)$$

$$\frac{\partial \overline{\rho} \widetilde{U} \varepsilon}{\partial z} + \frac{1}{r}\frac{\partial r\overline{\rho}\widetilde{V} \varepsilon}{\partial r} = \frac{1}{r}\frac{\partial}{\partial r}\left(r\frac{\mu_{eff}}{\sigma_\varepsilon}\frac{\partial \varepsilon}{\partial r}\right) + \overline{\rho}\frac{\varepsilon}{k}\left(C_1 P - C_2 \varepsilon\right)$$

$$P = \mu_{eff}\left(\frac{\partial \widetilde{U}}{\partial r}\right)^2$$

$$\mu_{eff} = \mu_l + \frac{C_\mu \bar{\rho} k^2}{\varepsilon}$$

$$C_1 = 1.4 - 3.4 \left(\frac{k}{\varepsilon} \frac{d\tilde{U}}{dz} \right)^3_{cl}$$

C_μ=0.09, C_2=1.9, σ_k=1, and σ_ε=1.3

The version of the k-ε turbulence model given above is a modification of the typically implemented variant of the k-ε turbulence model (C_1=1.44, C_2=1.92) to take account of the round jet/ plane jet anomaly, [23] where the spreading rate of round jets tends to be over predicted by the 'standard' version of the turbulence model. This is a well known limitation of most two equation turbulence models and 2nd moment closure models unless some modification is introduced to account for the reduced spreading rate. Indeed the 2nd moment closure model of Jones and Mussonge [24] was also applied to the jet fires considered here with little or no improvement. The modification to the k-ε model introduced above is due to Morse, [25] and has been used successfully in previous rim-stabilised fire simulation, [25]. The axisymmetric correction is used here as it gives an appropriate balance between model complexity and predictive capability. In addition a further modification to the turbulence model to account for buoyancy induced turbulence was implemented, [26] but ultimately rejected as the improvement in the mean temperature field was marginal at best.

Turbulent Combustion Model

The turbulent combustion model is a laminar flamelet combustion model, with two flamelet libraries, one for combustion and the other for isothermal mixing. Combustion is assumed to be infinitely fast with a prescribed probability density function, a β function, [27]. The shape of the β function at any spatial location is determined by a conserved scalar, the mixture fraction f and its variance f''^2, which are calculated using modelled transport equations, [11]. The combusting flamelet is calculated using a laminar counter flow non-premixed combustion simulation using a detailed kinetic scheme at a strain rate of 90 sec^{-1}, [11]. Any mean property can be calculated as a weighted average of the burning and isothermal mixing flamelet weighted by the pdf and integrated over instantaneous mixture fraction,

$$\tilde{\varphi} = P_d P_b \int_0^1 P(f)\varphi_b(f)df + (1 - P_d P_b)\int_0^1 P(f)\varphi_m(f)df$$

where P_b is a probability of burning defined below and P_d is a probability that the axial location is above the fluctuating flame base.

$$P_d = \int_0^\infty P_{base}(z > z_L)dz_L$$

Sanders and Lamers prescribe the pdf for the location of the instantaneous flame base, z_L to have a triangular shape, the apex located at the mean lift-off height and the base of the triangle is taken to be five diameters. It should be noted that this is an assumption of convenience rather than one based on observation, however a sensitivity study has shown that the overall flame structure is insensitive to this aspect of the model. The mean density and mean adiabatic temperature are given by the relations,

$$\bar{\rho} = \left[\frac{P_d P_b}{\int_0^1 P(f)\rho_b(f)df} + \frac{1 - P_d P_b}{\int_0^1 P(f)\rho_m(f)df} \right]^{-1}$$

$$\bar{T}_{adia} = P_d P_b \bar{\rho}_b \int_0^1 P(f)\frac{T_b(f)}{\rho_b(f)}df + (1 - P_d P_b)\bar{\rho}_m \int_0^1 P(f)\frac{T_m(f)}{\rho_m(f)}df$$

To account for radiation heat loss a transport equation for a specific enthalpy perturbation is solved,

$$\frac{\partial \bar{\rho}\tilde{U}\Delta h}{\partial z} + \frac{1}{r}\frac{\partial r\bar{\rho}\tilde{V}\Delta h}{\partial r} = \frac{1}{r}\frac{\partial}{\partial r}\left(r\frac{\mu_{eff}}{\sigma_{\Delta h}}\frac{\partial \Delta h}{\partial r} \right) + 4K_a \sigma\left(\bar{T}^4 - T_{amb}^4 \right)$$

where radiation heat loss is introduced using the optically thin approximation, [28]. The absorption coefficient, K_a is adjusted to gain agreement between the model and laboratory scale jet fire temperature measurements. The optically thin approximation is valid for laboratory scale methane jets. This approach has been used successfully in other computational studies [11, 12]. The mean temperature is then calculated as,

$$\bar{T} = \bar{T}_{adia} - \frac{\Delta h}{\sum_i Y_i C_{p,i}}$$

Y_i is the mass fraction of species i and the specific heat at constant pressure, $C_{p,i}$ is evaluated from curve fits in temperature to JANNAF thermodynamic property tables for each species, [29]. To close the system the probability of burning and the mean lift-off height must be modelled. The probability of burning is given by,

$$P_b = \int_0^{s_q} P(s)ds$$

s is the strain rate, s_q is the quenching strain rate and $P(s)$ is a quasi Gaussian pdf for the strain rate. Sanders and Lamers [4] give a quench strain rate of 565 sec^{-1} derived from an analysis of diluted methane-air counter flow diffusion flames. The strain rate can either be taken to be the strain rate of the small-scale turbulence,

$$s = C_{s,1}\left(\frac{\varepsilon}{2\nu_l}\right)^{1/2}$$

Or the strain rate of the large-scale turbulence.

$$s = C_{s,2}\frac{\varepsilon}{k}$$

Where $C_{s,1}$ and $C_{s,2}$ are calibration constants. The laminar dynamic viscosity is given by Sutherland's law, the constants in the formula can be found in Kalghati [2]. The mean lift-off height is prescribed using percolation theory, [16] and the probability of burning on the stoichiometric contour,

$$z_L\left(P_b = P_c\right)$$

$$s\Big|_{r=r_{st}} = \frac{s_q}{P_c\,\pi^{1/2}}$$

the above equation is an approximation to the error function and implicitly gives the percolation threshold, P_c, see Sanders and Lamers[4] for more details of the lift-off model.

As stated above the combustion model implemented is the one proposed by Sanders and Lamers, with some crucial differences that ultimately effects the overall conclusions of this article. It is therefore of interest to consider the differences

between the mathematical models described above and Sanders and Lamers approach. The main differences are the model described above includes radiation heat loss via the specific enthalpy perturbation transport equation and the turbulence model implemented accounts for the round jet/plane jet anomaly, [23]. These differences in model basis modify the predicted mean temperature field, and the turbulence fields. To appreciate the importance of taking account of the reduced spreading rate in round jets compared to planar jets Figure 1 shows the predicted and measured temperature field at three downstream locations for a jet fire. This is a rim-stabilised methane jet fire measured by Jeng et al. [10], the jet has a source diameter of 5 mm and a source velocity of 49.8 m/s giving a Reynolds number of 11,700. For each axial measuring station two predictions are shown, one using the round jet correction and the other using the standard turbulence model constants. The important difference between the two model predictions is the different spreading rate, with the corrected model giving more accurate predictions of the mean temperature field. There is some evidence for the over prediction of the spreading rate by Sanders and Lamers model, Figure 2 in [4] where the predicted radial position of the stoichiometric concentration is compared with Horch's data [30], good agreement is exhibited between Sanders and Lamers model and Horch's measurements for the first 20 diameters after which the agreement deteriorates.
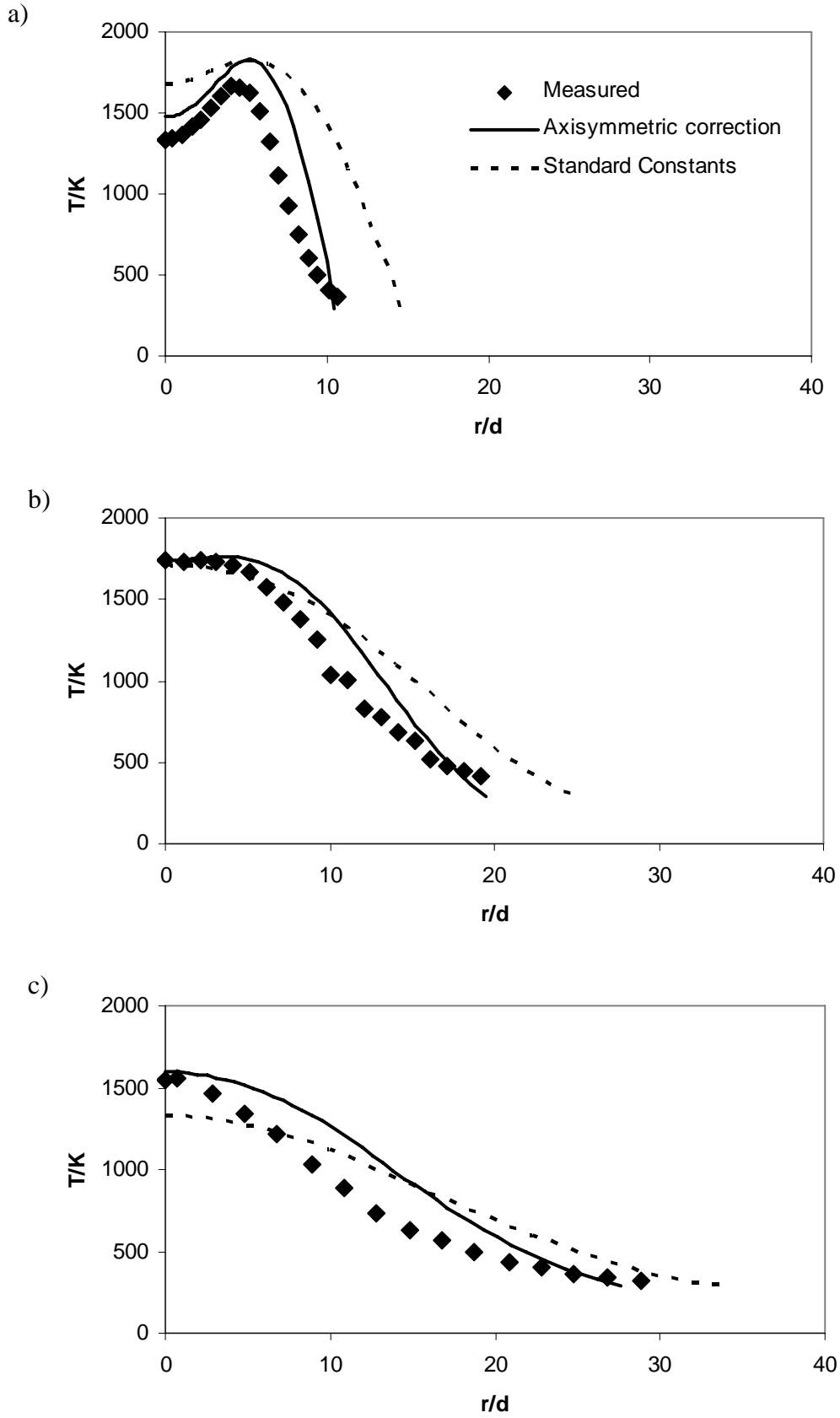
a)

b)

c)

Figure 1. Radial distributions of mean temperature at a) *z/d*=52.5, b) *z/d*=102 and c) *z/d*=150.

11

A third lift-off model is considered, based on a correlation for lift off height using a turbulence time-scale threshold.

$$z_L\left(\frac{k}{\varepsilon} \geq 5.E-3\right)$$

The turbulence time-scale is evaluated on the jet axis. This lift-off model is considered here as it is consistent with a parabolic flow model without modification and has been used in the past to predict the lift-off height of methane jet fires in a cross-flow, [27, 31-33]. The turbulence time-scale correlation was derived by Chakravarty et al., [34]. In this model the transition from no reaction to combustion is instantaneous at the lift-off height.

Boundary Conditions and Numerical Parameters

In all of the simulations presented below the bulk inlet conditions are given by the nozzle diameter and the average source velocity. The mean stream-wise velocity distribution and radial velocity distribution are taken to be consistent with fully developed pipe flow, that is a 1/7th power law is prescribed for the stream-wise velocity distribution and zero for the radial velocity component. Nozzle exit turbulence profiles are given by the formulae,

$$\frac{\sqrt{k_0}}{U_0} = 0.05$$

$$l_t = \frac{\min\left(\kappa\left(\frac{d}{2}-r\right), 0.1\frac{d}{2}\right)}{C_\mu^{0.75}}$$

$$\varepsilon_0 = \frac{k_0^{1.5}}{l_t}$$

For all simulations in this article 40 control volumes in the radial co-ordinate direction spanning the jet radius are used to calculate the flame structure, with a maximum fractional step in the axial direction of less than 2% of the radial control volume spacing. A number of simulations using 80 control volumes were also completed to confirm that the predictions presented are independent of further mesh refinement. It

is estimated that the predicted lift-off heights are within 2% of the fully mesh converged values.

Thermal Radiation Modelling

The external radiation heat flux distribution is modelled using a variant of the discrete transfer method, [35], modified using staggered ray meshes, [36, 37] to minimise the ray effect, [38]. Spectral emission from the fire is modelled using a statistical narrow band model, RADCAL, [39]. In the predictions of the external radiation heat flux presented in the following sections the spectrally integrated intensity is evaluated from integrations over the spectral window, 1µm- 1000µm with approximately 300-400 narrow bands. The predicted heat flux distributions are evaluated with 768 rays per receiver. 768 rays/ receiver was found to be sufficient for the predicted radiation heat flux distributions to be independent of further ray refinement, as increasing the number of rays used to 3072 rays/ receiver changed the flux by less than 5%.

Description of the Numerical Algorithm

When considering how a lifted flame differs from a rim-stabilised flame in the context of the mathematical model described above, the key difference is the composite probability of burning field,

$$P_{burn} = P_b\, P_d$$

In a rim-stabilised flame P_{burn} is one everywhere, whereas in a lifted flame this takes a value between zero and one. Zero below the lift-off region, between zero and one in the lift-off region and one above it. Therefore an algorithm based on a "guess and correct" approach for the composite probability of burning field suggests itself as one way of extending a parabolic flow model suitable for simulating rim-stabilised jet fires to simulate lifted jet fires. An overview of the algorithm in the form of a flow chart is given in Figure 2. To initialise the process some estimate of the composite probability of burning field must be prescribed. There are a number of possibilities, for example the fire could start off as being rim-stabilised, hence the initial composite probability of burning field could be set to one everywhere. An alternative choice is to prescribe the jet to be isothermal, with a composite probability of burning of zero

everywhere. Both options have some appeal as in the initial rim-stabilised fire approach ($P_{burn,0}=1$), this is how a lifted jet fire would initiate, alternatively the analysis of Pitts [3] and Sanders and Lamers [4] work on isothermal jets indicates that the non-reacting isothermal region upstream of the flame base is important in the flame stabilisation process, favouring the second approach ($P_{burn,0}=0$).
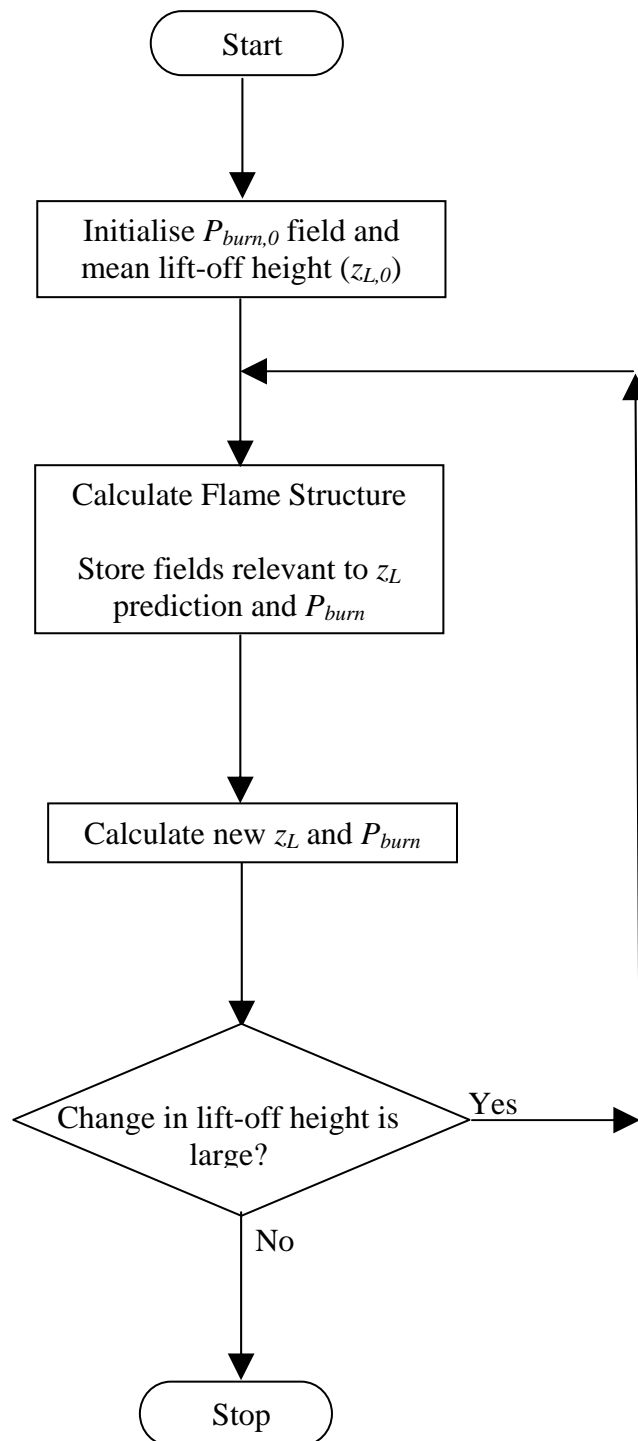

Figure 2. Flow chart of the lifted let fire methodology.

Once the composite probability of burning field is prescribed, an estimate of the flame structure can be calculated by running the parabolic flow model. As the flame structure is calculated flow fields required to estimate the lift-off height and the composite probability of burning field, such as the mean mixture fraction, mean temperature, turbulence kinetic energy, and the dissipation rate of the turbulence kinetic energy, are stored. Once the flame structure is complete, a new estimate of the lift-off height is calculated and the composite probability of burning field recalculated. If the change in lift-off height is small the algorithm is terminated otherwise the flame structure is recalculated and the process continues.

Large-Scale Strain Rate

In the description given above there are a number of issues identified or statements made that require further clarification? Figure 3 shows the convergence history for four simulations. The relative change in mean lift-off height is plotted against the iteration number. The jet fire simulated is the same in each case, (nozzle diameter 8mm, initial jet velocity of 71 m/s), for two of the simulations the large-scale strain rate sub-model is used, with different initial composite probability of burning fields and for the other two simulations the small-scale strain rate sub-model is used, again with two different initial composite probability of burning fields. In the convergence histories labelled as 'hot' start the initial guess for the composite probability of burning is one everywhere. The convergence histories labelled as 'cold' start the initial guess for the composite probability of burning is zero everywhere. Considering the simulations using the large-scale strain rate sub-model little sensitivity to the initial guess for the composite probability of burning is shown. The cold start simulation is marginally superior. Note that convergence is monotonic for the first twenty iterations after which round-off error prevents further convergence. However the differences in predicted lift-off heights for successive iterations is less than 0.01% and changes of less than 1% are sufficient for the lift-off height to be converged to the visual resolution of Figure 4. In Figure 4 the lift-off height as a function of iteration number is shown for the four simulations. Figure 3 and Figure 4 taken together suggest the algorithm takes around 5-6 iterations to converge when the large-scale strain rate sub-model is used in the lift off model.
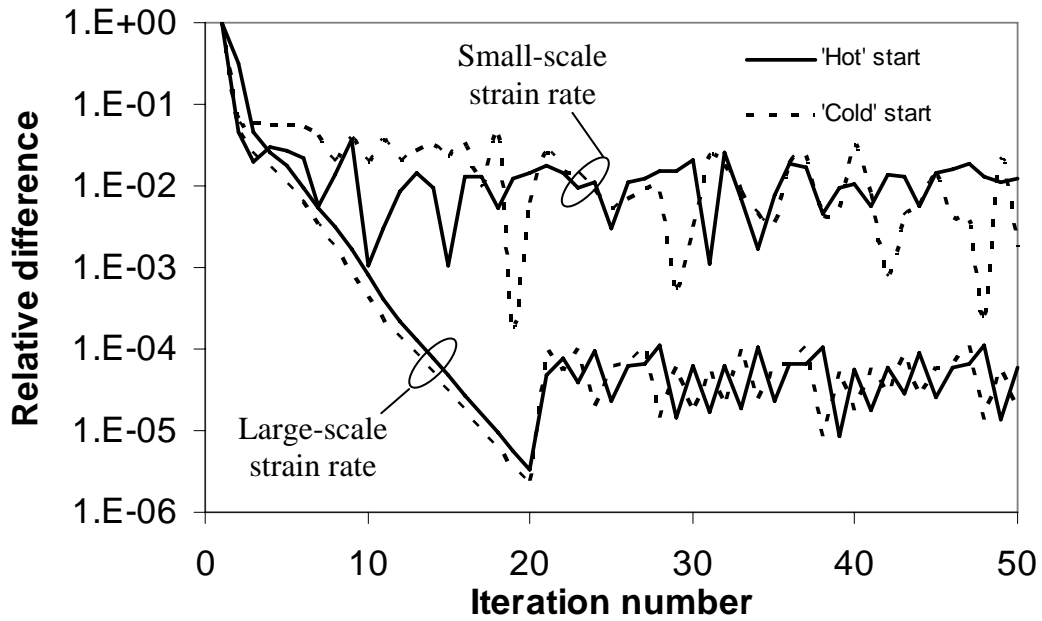
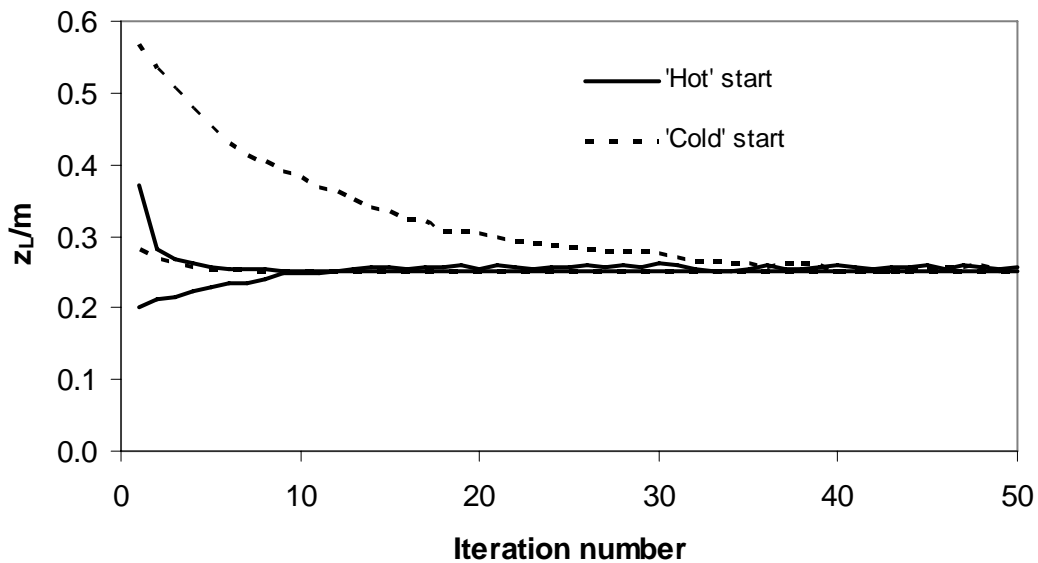Figure 3. Convergence histories for a lifted methane jet fire.

Figure 4. Predicted lift-off height as a function of iteration number.

Small-Scale Strain Rate

Considering the convergence histories for the small-scale strain rate simulations, the situation is less satisfactory. Monotonic convergence occurs for the first five iterations, after which no further convergence is achieved, with the change in lift-off height tending to approximately cycle through three different values all within 1% of

each other. The poor convergence behaviour of the simulations using the small-scale strain rate sub-model is believed to be due to its dependence on the dissipation rate of turbulence and the kinematic viscosity. These two properties are weakly correlated and when the lift-off height changes these two properties respond differently to the change in the mean temperature field. This convergence problem is lessened when more control volumes are introduced in the radial co-ordinate direction, with of course an increase in computational cost. The large-scale strain rate sub-model does not suffer from this problem as its dependency on turbulence parameters alone means that it responds in a consistent way to changes in the mean temperature field brought about by changes in the predicted mean lift-off height.

The small-scale strain rate simulations exhibit sensitivity to the initial composite probability of burning although both the hot and cold start simulations ultimately converge to the same lift-off height. The reason for the sensitivity can be explained by considering the predicted lift-off height as a function of iteration number, see Figure 4. For the small-scale strain rate simulation with a cold start, the first estimate of the mean lift-off height is over twice the converged value and on successive iterations decreases to the mean lift-off height, taking approximately forty iterations to reach it. Figure 4 also shows that false convergence is possible if just the change in mean lift-off height for successive iterations is used to monitor convergence. Comparing Figure 3 with Figure 4, for the small-scale strain rate simulation with a cold start, Figure 3 suggests that convergence is achieved in approximately twenty iterations if a convergence criterion of 1% change in lift-off height in successive iterations is prescribed; whereas in Figure 4 it is clear that convergence requires at least forty iterations.

Lift-off Height Model Calibration

Similar to Sanders and Lamers [4] the lifted jet fire model is calibrated using Wittmer's measurements of lift-off height for a methane jet with an initial velocity of 71 m/s and a nozzle diameter of 8 mm. Fitting the models to this data gives values of

$C_{s,1}$=0.33 and $C_{s,2}$=6

for the calibration constants in the strain rate sub-models. Sanders and Lamers only calibrated the small-scale strain rate sub-model for combusting jet simulations, giving a value of $C_{s,1}=0.27$. For the large-scale strain rate sub–model Sanders and Lamers give a calibration constant of $C_{s,2}=6.4$ but this was using isothermal jet simulations to predict the lift-off height. Sanders and Lamers did not calibrate the large scale strain rate model using combusting jet simulations due to the large computational cost of using an elliptic solver. The calibration constants used here are of the same order as those given by Sanders and Lamers, the differences are due primarily to the variant of the k-ε turbulence model used and the numerical resolution of the simulations.

Model Predictions

Figure 5 shows a comparison of the measured and predicted mean stream-wise velocity along the axis for the lifted jet fire used to calibrate the strain rate sub-models. Three predictions are shown, one using the turbulent time-scale sub-model for the lift-off height, a prediction using the large-scale strain rate sub-model and a prediction using the small-scale strain rate sub-model. Below the lift-off region all three models are identical as expected; further downstream the difference between the three models is small. Overall all three models agree with the measurements, the turbulent time-scale model giving slightly better agreement. For convenience Sanders and Lamer's prediction of mean stream-wise velocity using the small-scale strain rate model is also shown in Figure 5. Sanders and Lamer's prediction has a noticeable spike in the axial velocity at the lift-off height. Sanders and Lamers suggest this is due to the acceleration of the flow at the flame base because of the hot gas expansion due to initiation of combustion. The flow would accelerate to some degree due to the hot gases expanding, however this is not consistent with Wittmer's measurements although the spacing between measuring stations may be too far apart to capture the spike, if it were present.
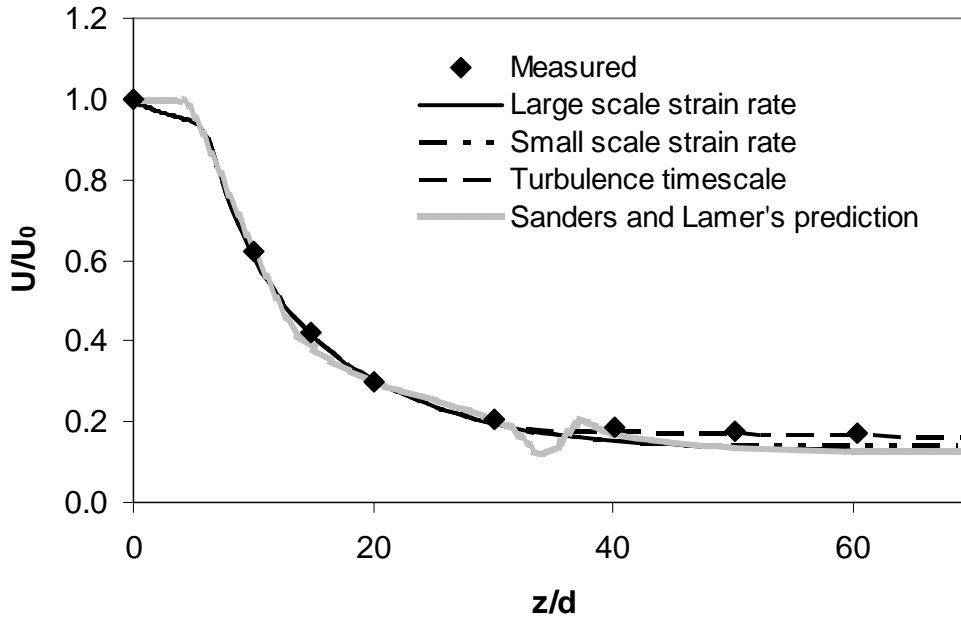
Figure 5. Stream-wise velocity on the jet axis (d=8mm, U_0=71 m/s).

The predicted and measured lift-off height as a function of source velocity is shown in Figure 6. Again three predictions are shown, the lift-off height based on the turbulence time-scale, and the lift-off height predicted using the small-scale and large-scale strain rate sub-models. The turbulence time-scale model gives a reasonable approximation of the lift-off height, however it should be noted that if this model were recalibrated to predict the high speed jet fire then its agreement for the other jet fires would worsen. Of the other two predictions the large-scale strain rate model gives the closest agreement to the measured lift-off height. The error for the lifted jet with a source velocity of 40 m/s using the large-scale strain rate sub-model is less than 15% compared to the small-scale strain rate model prediction, where the error is over 30%. Perhaps a more useful measure of agreement is a comparison of the gradient of the lines,
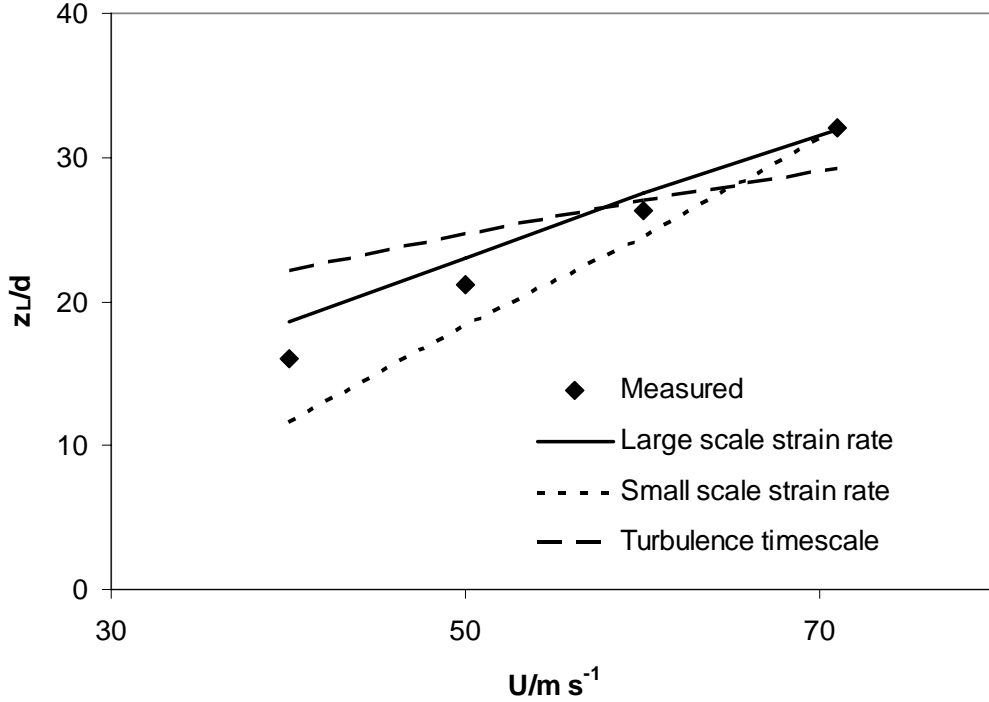
$$\frac{d\,z_L}{dU}$$

19

Figure 6. Lift-off height vs. source velocity.

The measured gradient is 4.13×10^{-3} sec compared to the predicted gradient of 3.45×10^{-3} sec using the large-scale strain rate sub-model, 5.2×10^{-3} sec using the small-scale strain rate and 1.84×10^{-3} sec for the predicted lift-off heights based on the turbulence time-scale model.

As mentioned above Sanders and Lamers compared the two strain rate sub-models ability to predict Wittmer's lift-off data and based on isothermal simulations concluded the small-scale strain rate was the superior of the two strain rate sub-models. To investigate the difference in conclusion between Sanders and Lamers, [4] and the present work, the turbulence model constants, C_1 and C_2 were changed to the values used by Sanders and Lamers and the strain rate sub-models recalibrated. The good agreement of the predicted lift-off height using the small-scale strain rate sub-model with Wittmer's data and the under prediction of the gradient, dz_L/dU for the large-scale strain rate sub-model was reproduced; see Figure 3 in [4]. However it must be emphasised the turbulence model constants used by Sanders and Lamers are not appropriate for axisymmetric free jets as discussed above.

Figure 7 shows the predicted temperature field at the flame base for all three lift-off models. The predicted temperature field where the turbulence time-scale threshold is used to predict the lift-off height is unrealistic in that the combustion model takes no account of the fluctuating nature of the flame base hence the step change in temperature at the flame base. The other two predicted temperature fields are more realistic in that no jump in temperature exists. Figure 8 shows the temperature field for the whole flame for all three lift-off models. In each case the temperature contours plotted are the same showing that the temperature field downstream of the lift-off region is insensitive to the way the lift-off region is modelled.
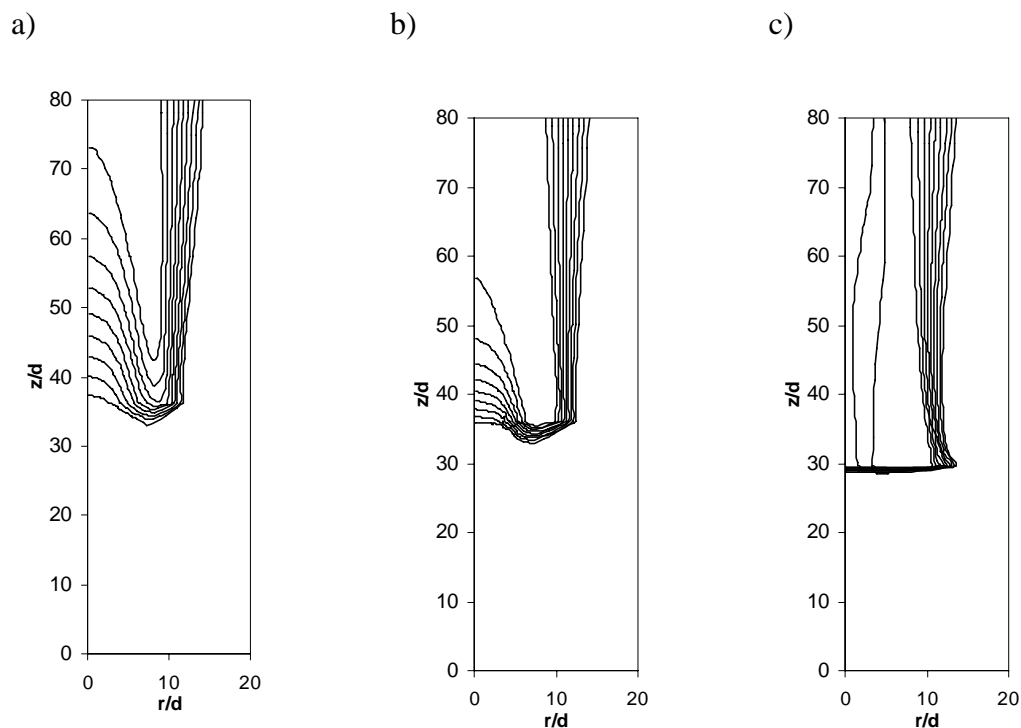
a)　　　　　　　　　　　　　　b)　　　　　　　　　　　　　　c)

Figure 7. Mean temperature field in the lift-off region, a) Large-scale strain rate prediction, b) Small-scale strain rate prediction, and c) turbulence time-scale prediction.
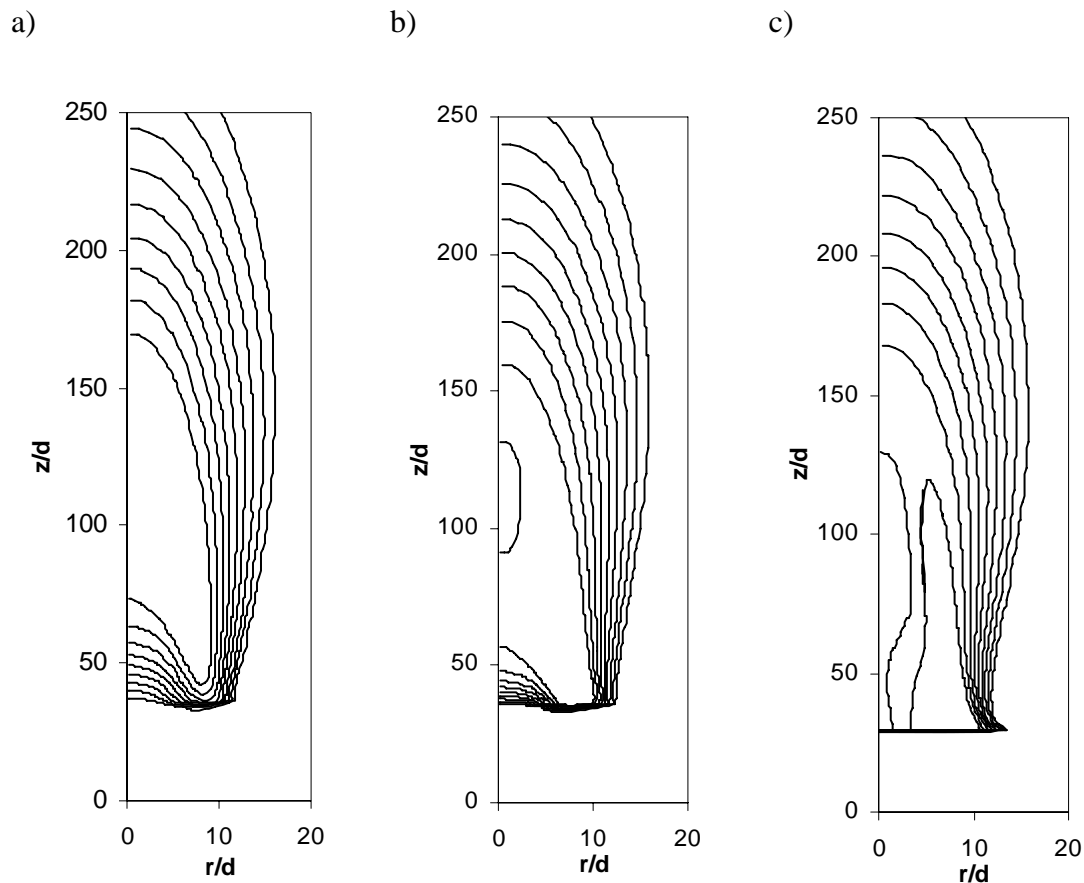
Figure 8. Mean temperature field. a) Large-scale strain rate prediction, b) Small-scale strain rate prediction, and c) turbulence time-scale prediction.

Radiation Field of a Lifted Jet Fire

One final consideration is the influence of the lift-off model on the received radiation field surrounding a jet fire. This is of interest as in many applications the flame structure is only of interest as a requirement for evaluating the received radiation field surrounding the fire. As the predicted mean temperature fields downstream of the lift-off region are similar for all three simulations, see Figure 8, the thermal radiation distribution in the far field should be similar. Figure 9 confirms this is the case. The differences in radiation heat flux distributions are consistent with the different mean temperature distributions in the lift-off region. In most safety applications it is the far field radiation heat flux distribution that is of major concern. The simulations in this paper suggest that the mean temperature field in the lift-off region is only important if

the near field thermal radiation distribution is of interest, such as if feedback to a flare tip were an issue.
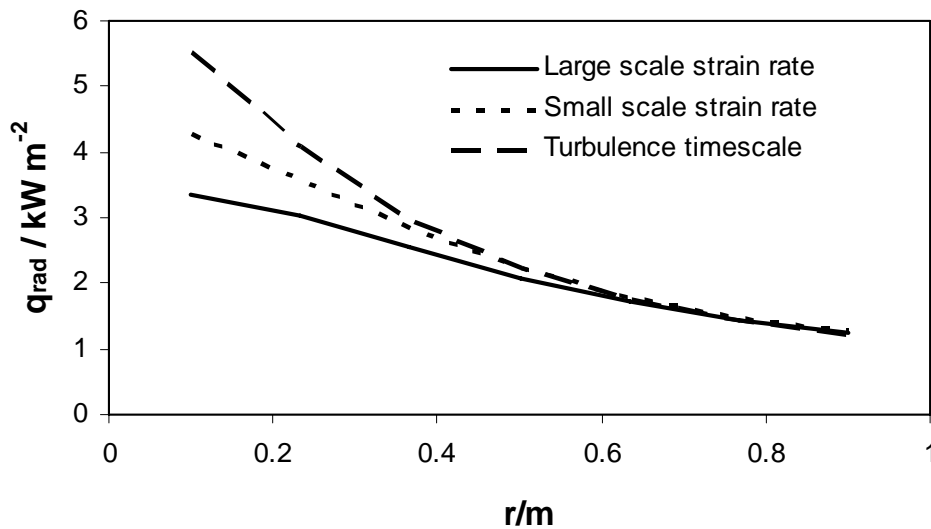

Figure 9. Heat flux distribution in a horizontal plane through the nozzle surrounding a jet fire.

Conclusion

In this article an algorithm for calculating the flame structure of lifted jet fires is presented. The algorithm is based on an extension of a fire model used to simulate rim-stabilised flames. An important characteristic of the lifted jet fire methodology is the flame structure is calculated using the boundary layer approximation. The advantage of this is finite volume mesh independent predictions of the mean flow fields can be calculated on readily available computer resources. The simulations presented here typically required of the order of 5 minutes run-time on a PC with a 450 MHz Pentium III processor. This has allowed a rigorous calibration of the lift-off models considered.

Three lift-off models were implemented and evaluated. The simplest uses a turbulence time-scale threshold to determine the lift-off height. This model is consistent with the boundary layer equations and can be implemented easily, but leads to unrealistic predictions of the mean temperature in the lift-off region. The other two lift-off models were formulated by Sanders and Lamers, [4] and are based on laminar

flamelet quenching for the flame stabilisation mechanism at the flame base. The two lift-off models are differentiated by the strain rate sub-model implemented. One is a small-scale strain rate sub-model; whereas the other is a large-scale strain rate sub-model. The use of the boundary layer equations means the lift-off models' calibration is rigorous. The lift-off models were evaluated by comparing predicted lift-off predictions and measurements taken by Wittmer. In this study the large-scale strain rate sub-model proved to be more accurate and the most numerically stable of the two strain rate sub-models. This is in contradiction to Sanders and Lamers who favour the small-scale strain rate sub-model.

The major difference between Sanders and Lamers analysis and the present article is the turbulence model implemented. The use of an axisymmetric correction to the turbulence model proved critical in evaluating the capabilities of the lift-off models. The next step is to validate the lift-off models using a wider range of measurements, both other lift-off data and detailed measurements of the mean temperature and chemical species in the lift-off region. This task is in hand and will be reported in a subsequent publication.

Finally the influence of the lift-off model on the external radiation heat flux distribution was considered. It was found the radiation heat flux distributions in the far field were insensitive to the lift-off model implemented, consistent with the prediction of the mean temperature field calculated using each lift-off model.

Acknowledgements

References

1. Gollahalli, S.R., Savas O., Huang, R.F. and Rodriquez Azara J.L., Structure of attached and lifted gas jet flames in hysteresis region, Twenty First Symposium (International) on Combustion, pp. 1463-1471, The Combustion Institute, Pittsburgh, 1986.

2. Kalghatgi, G.T., Lift-off heights and visible lengths of vertical turbulent jet diffusion flames in still air, Combust. Sci. and Tech., vol. **41**, 17-29, 1984.

3. Pitts, W.M., Importance of isothermal mixing processes to the understanding of lift-off and blowout of turbulent jet diffusion flames, Combust. Flame, vol. **76**, 197-212, 1989.

4. Sanders, J.P.H. and Lamers A.P.G.G., Modeling and calculation of turbulent lifted diffusion flames, Combust. Flame, vol. **96**, 22-33, 1994.

5. Muller, C.M., Breitbach. H. and Peters N., Partially premixed turbulent flame propagation in jet flames, Twenty Fifth First Symposium (International) on Combustion, pp. 1099-1106, The Combustion Institute, Pittsburgh, 1994.

6. Birch, A.D. and Hargrave, G.K., Lift-off Heights in underexpanded natural gas jet fires, Twenty Second Symposium (International) on Combustion, pp. 1463-1471, The Combustion Institute, Pittsburgh, 1988.

7. Birch, A.D., Brown, D.R., Cook, D.K. and Hargrave, G.K., Flame stability in underexpanded natural gas jets, Combust. Sci. and Tech., vol. **58**, 267-280, 1988.

8. McCaffrey, B.J. and Evans, D.D., Very large methane jet diffusion flames, Twenty First Symposium (International) on Combustion, pp. 25-31, The Combustion Institute, Pittsburgh, 1986.

9. Chao, Y.C., Yuan, T., and Tseng, C.S., Effects of flame lifting and acoustic excitation on the reduction of NO_x emissions, Combust. Sci. and Tech., vol. **114**, 49-65, 1996.

10. Jeng, S.M., Chen, L.D. and Faeth, G.M., The structure of buoyant methane and propane diffusion flames, Nineteenth Symposium (International) on Combustion, pp. 349-358, The Combustion Institute, Pittsburgh, 1982.

11. Cumber P.S., Fairweather M, and Ledin S., Application of wide band radiation models to non-homogeneous combustion systems, International Journal of Heat and Mass Transfer, vol. **41**, 1573-1584, 1998.

12. Fairweather. M., Jones W.P., Ledin, S. and Lindstedt, P., Predictions of soot formation in turbulent non-premixed propane flames, Twenty Fourth Symposium (International) on Combustion, pp. 1067-1074, The Combustion Institute, Pittsburgh, 1992.

13. Jeng, S.M., Lai, M.C. and Faeth G.M., Nonluminous radiation in turbulent buoyant axisymmetric flames, Combust. Sci. and Tech., vol. **40**, 41-53, 1984.

14. Cumber P.S. and Fairweather M., Evaluation of flame emission models for combustion system simulation, submitted International Journal of Heat and Mass Transfer, 2004.

15. Vanquickenborne, L. and Van Tiggelen, A., The stabilisation mechanism of lifted diffusion flames, Combust. Flame, vol. **10**, 59-68, 1966.

16. Peters, N. and Williams F.A., Lift-off characteristics of turbulent jet flames, AIAA J, vol. **21**, 423-429, 1983.

17. Pitts, W.M., Assessment of theories for the behaviour and blow-out of lifted turbulent jet diffusion flames, Twenty Second Symposium (International) on Combustion, pp. 809-816, The Combustion Institute, Pittsburgh, 1988.

18. Peters N., Laminar diffusion flamelet models in non-premixed turbulent combustion, Prog. Eng. Combust. Sci., vol. **10**, 319-339, 1984.

19. Upatnicks A., Driscoll, J.F., Rasmussen, C.C. and Ceccio, S.L., Lift-off turbulent jet flames- Assessment of edge flame and other concepts using cinema-PIV, Combust. Flame, vol. **138**, 259-272, 2004.

20. Spalding, D.B., GENMIX: A general computer program for two-dimensional parabolic phenomena, Pergamon Press, Oxford, 1977.

21. Wang, H. and Chen, Y., PDF modelling of turbulent non-premixed combustion with detailed chemistry, Chemical Engineering Sci, vol. **59**, 3477-3490, 2004.

22. Barlow, R.S. and Frank, J.H., Effects of turbulence on species mass fractions in methane/ air jet flames, Twenty Seventh Symposium (International) on Combustion, pp. 1087-1095, The Combustion Institute, Pittsburgh, 1998.

23. Pope, S.B., An explanation of the turbulent round-jet/ plane-jet anomaly, AIAA J, **16**, 279-281, 1978.

24. Jones, W. and Musonge, P., Closure of the Reynolds stress and scalar flux equations, Phys Fluids, vol. **31**, 3589-3604, 1988.

25. Moss, J.B., Stewart, C.D. and Syed, K., Flow field modelling of soot formation at elevated pressure, Twenty Second Symposium (International) on Combustion, pp. 413-423, The Combustion Institute, Pittsburgh, 1988.

26. Hossain, M.S. and Rodi, W., Influence of buoyancy on the turbulence intensities in horizontal and vertical jets, Heat transfer and buoyant convection, Edited by D.B. Spalding and N. Afgan, Hemisphere publishing corporation, Washington, 1976, Vol. 1, 39-51.

27. Fairweather, M., Jones, W.P. Lindstedt, R.P. and Marquis, A.J., Predictions of a turbulent reacting jet in a cross-flow, Combust. Flame, vol. **84**, 361-375, 1991.

28. Siegel, R. and Howell, J.R., Thermal Radiation Heat Transfer, 3rd Edition, Hemisphere Publishing Corporation, 1992.

29. Chase, M.W., Davies, C.A., Downey, J.R., Frurip, D.J., McDonald R.A. and Syverud, A.N., 1985, JANAF Thermochemical Tables, 3rd Edition Journal Physical and Chemical Reference Data, vol. **14**, 1985.

30. Horch, K., PhD thesis, Universitat Karlsruhe, Germany, 1978.

31. Fairweather, M., Jones, W.P. and Lindstedt, R.P., Predictions of radiative heat transfer from a turbulent reacting jet in a cross-wind, Combust. Flame, vol. **89**, 45-63, 1992.

32. Cleaver, R.P., Cumber, P.S. and Fairweather M, Predictions of sonic jet fires, Combust. Flame, vol. **132**, 463-474, 2003.

33. Cook, D.K., Cumber, P.S., Fairweather, M. and Shemirani, F., Modelling free and impacting underexpanded jet fires, IChemE Symposium Series, No. 141, pp. 127-138, The Institution of Chemical Engineers, Rugby, 1997.

34. Chakravarty, A., Lockwood, F.C. and Sinicropi, G., The prediction of burner stability limits, Combust. Sci. and Tech., vol. **42**, 67-86, 1984.

35. Lockwood, F.C. and Shah, N.G., A new radiation solution method for incorporation in general combustion prediction procedures, Eighteenth Symposium (International) on Combustion, pp. 1405-1414, The Combustion Institute, Pittsburgh, 1981.

36. Cumber, P.S., Improvements to the discrete transfer method of calculating radiative heat transfer, International Journal of Heat and Mass Transfer, vol. **38**, 2251-2258, 1995.

37. Cumber P.S., Ray effect mitigation in jet fire radiation modelling, International Journal of Heat and Mass Transfer, vol. **43**, 935-943, 2000.

38. Chai, J.C., Haeok, S.L. and Patankar, S.V., Ray effect and false scattering in the discrete ordinates method, Numerical Heat Transfer, Part B, vol. **24**, 373-389, 1993.

39. Grosshandler, W.L., Radiative heat transfer in non-homogeneous gases: A simplified approach, International Journal of Heat and Mass Transfer, vol. **23**, 1447-1459, 1980.